Electronic Supplementary Information

Semisynthetic peptide-lipase conjugates for improved biotransformations

Oscar Romero, Marco Filice, Blanca de las Rivas, Cesar Carrasco-Lopez, Javier Klett, Antonio Morreale, Juan A. Hermoso, Jose M. Guisán, Olga Abian and Jose M. Palomo*

Table of contents

Experimental Section 3
Materials 3
Site-directed mutagenesis of BTL 3
Enzymatic activity assay 3
Cloning, expression, purification and immobilization of BTL variants 4
Peptides 4
Protection of thiol in BTL variants by 2-PDS 4
Chemical incorporation of tailor-made peptides on different BTL variants 5
Desulfurization reaction 5
MALDI-TOF-MS spectra 5
Circular dichroism 5
Fluorescence spectroscopy 6
Irreversible inhibition of BTL2 immobilized preparations by D-pNP 6
Kinetic parameters calculation 6
Acetylation of thymidine 6-7
Enzymatic hydrolysis of 3',5'-di-O-acetylthymidine (1) 7
Enzymatic hydrolysis of 3,4,6-tri-O-acetyl-glucal (4) 7
Enzymatic hydrolysis of dimethyl-3-phenylglutarate (6) 7-8
Determination of enantiomeric excess 8
Targeted molecular dynamics (MD) simulation 8
Local enhanced sampling (LES) 9
References 10
Supplementary Figures 11
Fig S1. SDS-PAGE of BTL-A193C 11
Fig S2. Characterization of BTL variants. 12
Fig S3. Surface structure of lid zone of BTL mutants.. 12

Fig S4. Characterization of BTL*-S196C-p2 conjugate 14
Fig S5. Characterization of BTL*-L230C-p2 conjugate 15
Fig S6. Irreversible inhibition by D-pNP 16
Fig S7. Time-evolution of RMSD and tRMSD values for the Targeted MD of BTL 17
Fig S8. Interaction network of the p1 tag within the modeled structure of the semisynthetic conjugated variant BTL*-A193C-p1 18
Fig S9. Comparison between the crystal structure of the active form of BTL and the semisynthetic conjugated variant BTL*-S196C-p2. 19
Fig S10. Interaction network of the p2 tag within the modeled structure of the semisynthetic conjugated variant BTL*-S196C-p2 20
Fig S11. Fluorescence spectra of the immobilized BTL variants. 21

Supplementary Tables 22
Table S1. Primers used to site-directed mutagenesis of BTL 22
Table S2. Different peptide sequences 23
Table S3. Regioselective hydrolysis of peracetylated thymidine 1 catalyzed by peptide-modified immobilized BTL2 mutants at pH 5 and 25ºC. 24
Table S4. Regioselective hydrolysis of peracetylated tymidine 1 catalyzed by peptide-modified immobilized BTL2 mutants at pH 7 and 25ºC. 25
Table S5. Regioselective hydrolysis of peracetylated glucal 4 catalyzed by peptide-modified immobilized BTL2 mutants. 26
Table S6. Desymmetrization of phenylglutaric acid dimethyl ester catalyzed different BTL-variants at pH 7.0. 27
Table S7. Kinetic parameters of different BTL immobilized preparations 27

Experimental Section

Materials

Sepharose® 4BCL activated with cyanogen bromide (CNBr) and Butyl-Sepharose® 4 Fast Flow were from GE Healthcare (Uppsala, Sweden), 2-dipyridyldisulfide (2-PDS), diethyl-p-nitrophenylphosphate (D-pNP), dithiothreitol (DTT), sodium borohydride, Triton® X-100, dimethylsulfoxide (DMSO), tris(dimethylamino)phosphine, Dimethyl 3-phenylglutarate (**6**), thymidine and p-nitrophenylbutyrate (pNPB), per-O-acetylated glucal (**4**) were from Sigma.

Site-directed mutagenesis of BTL

All site-directed mutagenesis experiments were carried out by PCR using mutagenic primers (Table S1). Briefly, to introduce the amino acid change, the corresponding pair of primers was used as homologous primer pair in a PCR reaction using a specific plasmid as template and Prime Start HS Takara DNA polymerase. The product of the PCR was digested with endonuclease *DpnI* that exclusively restricts methylated DNA.[1] *E. coli* DH10B cells were transformed directly with the digested product. The plasmid with mutated *btl* were identified by sequencing and then transformed into *E. coli* BL21 (DE3) cells to express the corresponding proteins. Firstly, C65S was created, and the resulting plasmid was used as template to create the double mutant C65S/C296S-BTL.[2] This plasmid was used as template to construct additional mutations (A193C, S196C, L230C) using different mutagenic primers (Table S1).

Enzymatic activity assay

The activities of the soluble and immobilized BTL variants were analyzed spectrophotometrically measuring the increment in absorbance at 348 nm produced by the release of p-nitrophenol (pNP) (ϵ = 5,150 M^{-1} cm^{-1}) in the hydrolysis of 0.4 mM *p*NPB in 25 mM sodium phosphate at pH 7 and 25 °C. To initialize the reaction, 0.05–0.2 mL of lipase solution or suspension was added to 2.5 mL of substrate solution. Enzymatic activity is given as micromole of hydrolyzed pNPB per minute per milligram of enzyme (IU) under the conditions described above.

Cloning, expression, purification and immobilization of BTL variants

The gene corresponding to the mature lipase from *G. thermocatenulatus* BTL was cloned into pT1 expression vector as previously described.[1,2] Cells carrying the recombinant plasmid pT1BTL2 were grown at 30 °C and over expression were induced by raising the temperature to 42 °C for 20 h. The enzyme was purified from *Escherichia coli* crude extract by interfacial adsorption on Butyl-Sepharose as previously described [3] (Fig.S1). The lipase was desorbed from the support adding 20 mL of 25 mM phosphate buffer pH 7 with 0.5% Triton X-100 (v/v) per gram of support. After that, the lipase was immobilized on CNBr-activated Sepharose at pH 7 in 25 mM sodium phosphate buffer for 1 h at 25ºC (>95% immobilization yields) with a final loading of 5 mg_{lip}/g_{cat}.[3] The remaining pNPB activity for the different immobilized BTL variants was more than 95% of the initial activity.

Peptides

Peptides (**p1**-**p4**, **p6**-**p8**) (Table S2) were purchased from Inbios (Italy). Peptide **p5** (Table S2) was synthesized by solid-phase strategy using Rink-amide linker and Fmoc chemistry.[4]

A peptide solution (0.5 mg/mL) was treated with sodium borohydride solution (2 mg/mL) in 25 mM sodium bicarbonate at pH 10.0 for 30 min in order to conserve the thiol group in a reductive form. After, the pH was adjusted to 7.0 with diluted HCl solution to destroy the remaining sodium borohydride.

Protection of thiol in BTL variants by 2-PDS

Different BTL variants (0.2 g of the immobilized form) were incubated in 2 ml of DTT solution (50 mM in 25 mM sodium phosphate at pH 8) for 30 min to avoid oxidation and permit the posterior disulfide exchange. After, the reduced biocatalysts were washed with distilled water until the DTT smell disappears.

Then 0.2 g of reduced BTL variants was added to 3 ml of 2-PDS solution (1.5 mM substrate in a mixture of DMSO (5%, v/v)-25mM phosphate buffer (95%, v/v) at pH 8.0) for 1 h. The cysteine PDS activation was followed spectrophotometrically by measuring the increase of the absorbance at 343 nm (by the release of 2-mercaptopyridine, which quickly tautomerizes into 2-thiopyridone) of the solution. A full modification was found in all BTL variants.[5]

Chemical incorporation of tailor-made peptides on different BTL variants

0.7 ml of peptide solution was dissolved in 2.3 mL of 500 mM sodium phosphate at pH 8. Then, 0.2 g of immobilized PDS-BTL variants was added. After 1 h, the modification was confirmed spectrophotometrically by measuring the increase of the absorbance at 343 nm. The catalyst was filtered (immobilized form) and washed with distilled water or dialyzed with four changes of distilled water (solution).

Samples were purified and concentrated by Amicon Ultra 10kDa (DyeEx columns from Qiagen) and characterized by MALDI-TOF. The BTL variants were analyzed by SDS-PAGE on 10% (w/v) polyacrylamide gels by Coomassie staining and fluorescence and CD.

Desulfurization reaction[6]

10 mL of a solution of 1.5 mM of Tris(dimethylamino)phosphine in 70 mM CAPS buffer pH 9.5 was added to 1.0 g of lipase-peptide conjugates immobilized preparations and maintained at room temperature for 16 h. Then was filtered and washed with distilled water. The thioether formation was confirmed by MALDI-TOF.

MALDI-TOF-MS spectra

MALDI-MS spectra of the different BTL variants and peptide conjugates were recorded in a Bruker MicroFlex (Bruker Daltonics) by using sinapic acid as matrix. 5 µL of pure protein sample (1 mg/mL) were mixed with 5 µl of a saturated sinapic solution (70:30 water/acetonitrile with 0.1% TFA final concentration). The mixture was pipeted on the target (1 µL) and dried at ambient temperature. We would like to thank Dra. Grazu from Instituto de Nanociencia de Aragón (INA) and Dr. Jesús Orduna and Ms Saviron from ICMA (Instituto de Ciencia de Materiales de Aragón) and Servicio de Espectrometria de masas del CEQMA in Zaragoza from MALDI-TOF analysis.

Circular dichroism

Circular dichroism (CD) spectra of the different BTL variants and peptide conjugates were recorded in a Chirascan spectropolarimeter (Applied Photophysics) at 25(±1)°C. Near-UV spectra were recorded at wavelengths between 250 and 310 nm in a 1 cm path-length cuvette, with 10 µM protein solutions in phosphate buffered saline, pH 7.2 (PBS; bioMerieux). Far-UV spectra were measured at wavelengths between 190 and

250 nm in a 1 mm path-length cuvette, with 2 μM protein solutions in the same buffer. Blank measurements were made with the appropriate buffer.

Fluorescence spectroscopy

Fluorescence measurements were performed in a Varian Cary Eclipse Fluorescence Spectrophotometer (Agilent Technologies) monitoring the intrinsic tryptophan fluorescence in the different BTL variants and peptide conjugates, using an excitation wavelength of 280 nm, with excitation and emission bandwidths of 5 nm, and recording fluorescence emission spectra between 300 and 400 nm. All spectroscopic measurements were made in water.

Irreversible inhibition of BTL2 immobilized preparations by diethyl-p-nitrophenylphosphate (D-pNP)

0.2 g of different BTL2 immobilized preparations were suspended in 4 mL of 25 mM sodium phosphate buffer solution at pH 7 and 25 °C with or without the presence of 0.5% of Triton X-100. Then, 1.5 mM of inhibitor (D-pNP) was added to this solution. The reaction was maintained until the activity–measured using pNPB assay- of the immobilized enzyme was zero.

Kinetic parameters calculation

K_m and K_{cat} values for the different BTL variants and corresponding conjugates in the hydrolysis of pNPB were calculated (Table S7).

Acetylation of thymidine

A suspension of thymidine (12 mmol, 2.9 g) in acetonitrile (1 mL/0.2 mmol of nucleoside) was treated with triethylamine (TEA, 4 equiv.) and acetic anhydride (4 equiv.) in the presence of a catalytic amount of 4-(dimethylamino) pyridine (DMAP). The resulting mixture was stirred at room temperature until the reaction was complete (TLC analysis) and was then diluted with chloroform and water (1:1). The organic phase was separated, washed with water (4x 20-50 mL) and dried (Na_2SO_4), filtered, and concentrated in vacuo The residue was purified by silica gel column chromatography (CH_2Cl_2 100% to CH_2Cl_2/MeOH, 98:2) to afford the 3',5'-di-O-acetylthymidine **1** (3.5 g, 90%). TLC (ethyl acetate/hexane, 7/3): R_f = 0.32. ^{1}H-NMR (400 MHz, [D_6]-DMSO, 25 °C): δ = 10.70 (s, 1 H, 3-NH), 7.50 (s, 1 H, 6-H), 6.10 (dd,

1 H, 1'-H), 5.10 (m, 1 H, 3'-H), 4.20-4.00 (m, 3 H, 4'-H, 5'-H), 2.80 (m, 2 H, 2'-H), 2.10-2.00 (s, 6 H, 2 OAc), 190 (s, 3 H, 5-H) ppm.

Enzymatic hydrolysis of 3',5'-di-O-acetylthymidine (1)

Substrate **1** (5 mM) was dissolved in a mixture of acetonitrile (5%, v/v) in 10mM sodium phosphate at pH 7.0 or 10mM sodium acetate at pH 5.0. 0.2 g of biocatalyst was added to 2 mL of this solution at 25°C. During the reaction, the temperature and the pH value was maintained constant using a pH-stat Mettler Toledo DL50 graphic. The degree of hydrolysis was analyzed by reverse phase HPLC (Spectra Physic SP 100 coupled with an UV detector Spectra Physic SP 8450). For these assays a Kromasil C18 (25× 0.4 cm, 5µmø) column was used and the following gradient program (A: mixture of acetonitrile (10%, v/v) in 10mM ammonium phosphate at pH 4.2; B: mixture of miliQ water (10%,v/v) in acetonitrile; method: 0-6 min 100% A, 6-14min 85% A to 15%B, 14-22 min 100% A, flow: 1.0 mL min-1). UV detection was performed at 260 nm. The unit of enzymatic activity was defined as micromoles of substrate hydrolyzed per minute per mg of immobilized protein. The monodeprotected 5-OH (**2**) and 3-OH (**3**) were used as pure standards. The retention time was 2.4 min for Thymidine, 9.4 min for **3** and 10.2 min **2** and 19 min for **1**.

Enzymatic hydrolysis of 3,4,6-tri-O-acetyl-glucal (4)

Substrate **4** (2.0 mM) was dissolved in a mixture of acetonitrile (3%, v/v) in 10mM sodium acetate at pH 5.0. 0.4 g of biocatalyst was added to 2 mL of this solution at 25°C. During the reaction, temperature and the pH value was maintained constant using a pH-stat Mettler Toledo DL50 graphic. The degree of hydrolysis was analyzed by reverse phase HPLC (Spectra Physic SP 100 coupled with an UV detector Spectra Physic SP 8450). For these assays a Kromasil C18 (25× 0.4 cm, 5µm ø) column was used and the mobile phase was acetonitrile (30%) in 10mM ammonium phosphate at a final pH value of 4.0. UV detection was performed at 220 nm. The unit of enzymatic activity was defined as micromoles of substrate hydrolyzed per minute per mg of immobilized protein. The retention time was 5.1 min for **5** and 18 min for **4**.

Enzymatic hydrolysis of dimethyl-3-phenylglutarate (6)

Substrate **6** (0.5 mM) was dissolved in 10 mM sodium phosphate or 10 mM sodium acetate at pH 7.0 and 5.0, respectively. Then 0.25 g of immobilized preparation was

added to 5 mL of this solution at 25°C. During the reaction, temperature and the pH value was maintained constant using a pH-stat Mettler Toledo DL50 graphic. The degree of hydrolysis was analyzed by reverse phase HPLC (Spectra Physic SP 100 coupled with an UV detector Spectra Physic SP 8450). For these assays a Kromasil C8 (25× 0.4 cm, 5μm ø) column was used and the mobile phase was acetonitrile (35%) in 10mM ammonium phosphate at a final pH value of 3.0. UV detection was performed at 225 nm. The unit of enzymatic activity was defined as micromoles of substrate hydrolyzed per minute per mg of immobilized protein. The retention time was 7.4 min for **7** and 22 min for **6**.

Determination of enantiomeric excess

The enantiomeric excess (ee) of the released monoester **7** was analyzed by chiral reverse phase HPLC. The column was a Chiracel OD-R, the mobile phase was an isocratic mixture of acetonitrile (20%, v/v) in 10 mM ammonium phosphate (80%, v/v) at pH 3. The detection of the compounds was performed at 210 nm. The retention time was 58.7 min for (R)-**7** and 63.2 min for (S)-**7**.

Targeted molecular dynamics (MD) simulation

The conformational transition from the closed/inactive to the open/active conformations for the bacterial thermoalkalophilic lipase was modelled using targeted MD technique as implemented in AMBER 11 suite of programs.[7-8] The models for the corresponding structures were taken from the PDB (PDB IDs 1JI3 and 2W22, respectively). Addition of missing hydrogen atoms and computation of the protonation state of ionizable groups at pH 6.5 were carried out using the H++ Web server,[9] which relies on AMBER parameters and finite difference solutions to the Poisson–Boltzmann equation. A salt concentration of 0.15 M and an internal and external dielectric constant of 4 and 80, respectively, were used. Atom types and charges for each atom were assigned according to AMBER ff10 force field.[10] Both systems were hydrated by using boxes containing explicit TIP3P water molecules[11] with added counter ions to maintain electro neutrality. Solvent molecules and counter ions were relaxed by energy minimization and then allowed to redistribute around the positional restrained structures during a 50 ps run at constant temperature (300 K) and pressure (1 atm). These initial harmonic restraints were gradually reduced in a series of progressive energy minimizations steps until they

were completely removed. The resulting systems were heated again from 100 to 300 K during 20 ps and allowed to equilibrate in the absence of any restraints for 1.0 ns during which system coordinates were collected every 2 ps for further analysis. The equilibrated structures were then used as the starting points for the targeted MD simulations lasting 5 ns. Periodic boundary conditions and the Particle Mesh Ewald methods were used to treat long-range electrostatic effects. The SHAKE algorithm was applied to all bonds and an integration step of 2.0 fs was used throughout.

The targeted MD method allows observing large scale conformational transitions between two known end point conformations of a protein, which are presently beyond the reach of atomistic MD simulations. This is accomplished by an additional steering force based on a mass-weighted RMSD with respect to reference target conformation that is applied in the force field as an extra harmonic potential energy term of the form in Eq. 1:

$$E = 0.5 \cdot k_r \cdot N \cdot (RMSD - tRMSD)^2 \qquad \text{Eq. 1}$$

where k_r is the force constant, N is the number of atoms, $RMSD$ is the mass-weighted root-mean-square deviation of the initial structure with respect to the target structure, and $tRMSD$ is the desired root-mean-square deviation value which gradually decreased to cero during the simulation. A force constant of 0.25 kcal mol^{-1} Å^{-2} over a period of 5.0 ns proved sufficient to find a low-energy path leading from the initial to the target structure (Fig. **S6**).

Local enhanced sampling (LES)

The targeted MD trajectory was visually inspected and the motions of ALA193 and SER196 residues were monitored, as these are the residues were peptides chains **p1** and **p2** will be attached. Two critical points were detected in which the attached peptides would unlikely yield to an active/open conformation due to steric clashes: at 3041 for ALA193 and at 2111 ps for SER196. ALA193 and SER196 were mutated to CYS in the structures corresponding to these points and finally, poly-phenylalanine and poly-aspartic chains were anchored using PyMOL.[12] The structures were relaxed by simulating them for a period of 50 ps at constant temperature (300 K) and pressure (1 atm). LES[13] simulation was performed selecting the added peptide chains for the enhanced sampling. Each LES simulation was carried out over a period of 500 ps with a cut-off distance for the non-bonded interactions of 15 Å.

References

1. C. Schmidt-Dannert, M.L. Rua, H. Atomi and R.D. Schmid. *Biochim. Biophys. Acta* 1996, **1301**, 105-114.

2. C.A, Godoy, B. de las Rivas, V. Grazú, T. Montes, J.M Guisán and F. López-Gallego. *Biomacromolecules* 2011, **12**, 1800-1809.

3. G. Fernández-Lorente, C. Godoy, A.A. Mendes, F. Lopez-Gallego, V. Grazu, B. de las Rivas, J.M. Palomo, J. Hermoso, R. Fernández-Lafuente and J.M Guisán. *Biomacromolecules.* 2008, **9**, 2553-2561.

4. X. Li, R. Higashikubo and J.-S. Taylor. *Bioconjugate Chem.* 2008, **19**, 50–56.

5. C.A. Godoy, B. de Las Rivas, M. Filice, G. Fernández-Lorente, J.M. Guisán and J.M. Palomo. *Process Biochem*. 2010, **45**, 534-541.

6. G.J.L. Bernardes, E. J. Grayson, S. Thompson, J. M. Chalker, J.C. Errey, F. El Oualid, T.D.W. Claridge and B.G. Davis. *Angew. Chem. Int. Ed.* 2008, **47,** 2244-2247.

7. D.A Case, T.E Cheatham III; T. Darden, H. Gohlke, R. Luo, K.M.Jr Merz, A. Onufriev, C. Simmerling, B. Wang and R.J. Woods. *J Comput Chem* 2005, **26**, 1668-1688.

8. D.A Pearlman, D.A. Case, J.W Caldwell, W.S Ross, T.E Cheatham III, S. DeBolt, D. Ferguson, G. Seibel and P. Kollman. *Comput. Phys. Commun.* 1995**, 91**, 1-41.

9. J.C Gordon, J.B Myers, T. Folta, V. Shoja, L.S Heath and A. Onufriev. *Nucleic Acids Res* 2005, **33** (Web Server issue), W368-W371.

10. J. Wang and P.A Kollman. *J Comput Chem* 2001**, 22**, 1219-1228.

11.W.L Jorgensen, J. Chandrasekhar, J.D Madura, R.W Impey and M.L Klein. *J. Chem. Phys* 1983, **79**, 926-935.

12. *The PyMOL Molecular Graphics System, Version 1.2r3pre, Schrödinger, LLC. (www.pymol.org).*

13. R. Elber and M. Karplus. *J. Am. Chem. Soc.* 1990, **112**, 9161-9175.

Supplementary Figures

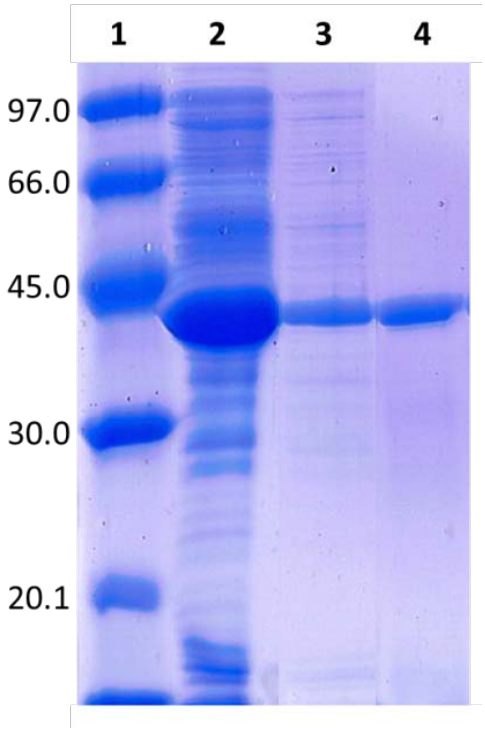

Fig S1. SDS-PAGE of BTL*-A193C. Lane 1: molecular weight marker (KDa); Lane 2: BTL extract; Lane 3: Absorbed on Butyl-Sepharose; Lane 4: Desorbed from Butyl-Sepharose. All BTL variants were purified with the same protocols and similar results.

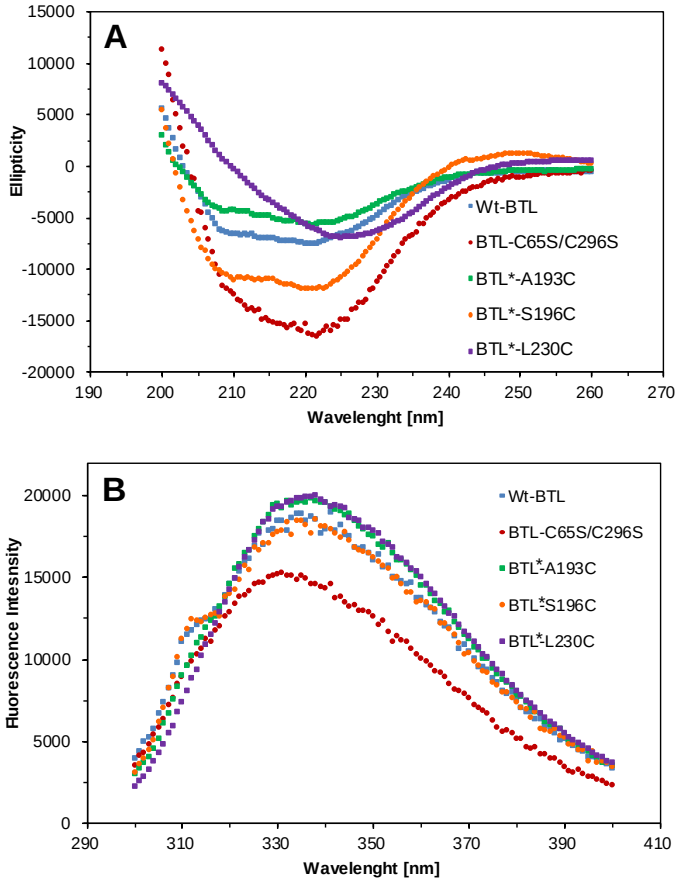

Fig S2. Characterization of BTL variants. (A) Far-UV CD spectra; (B) Fluorescence spectra.

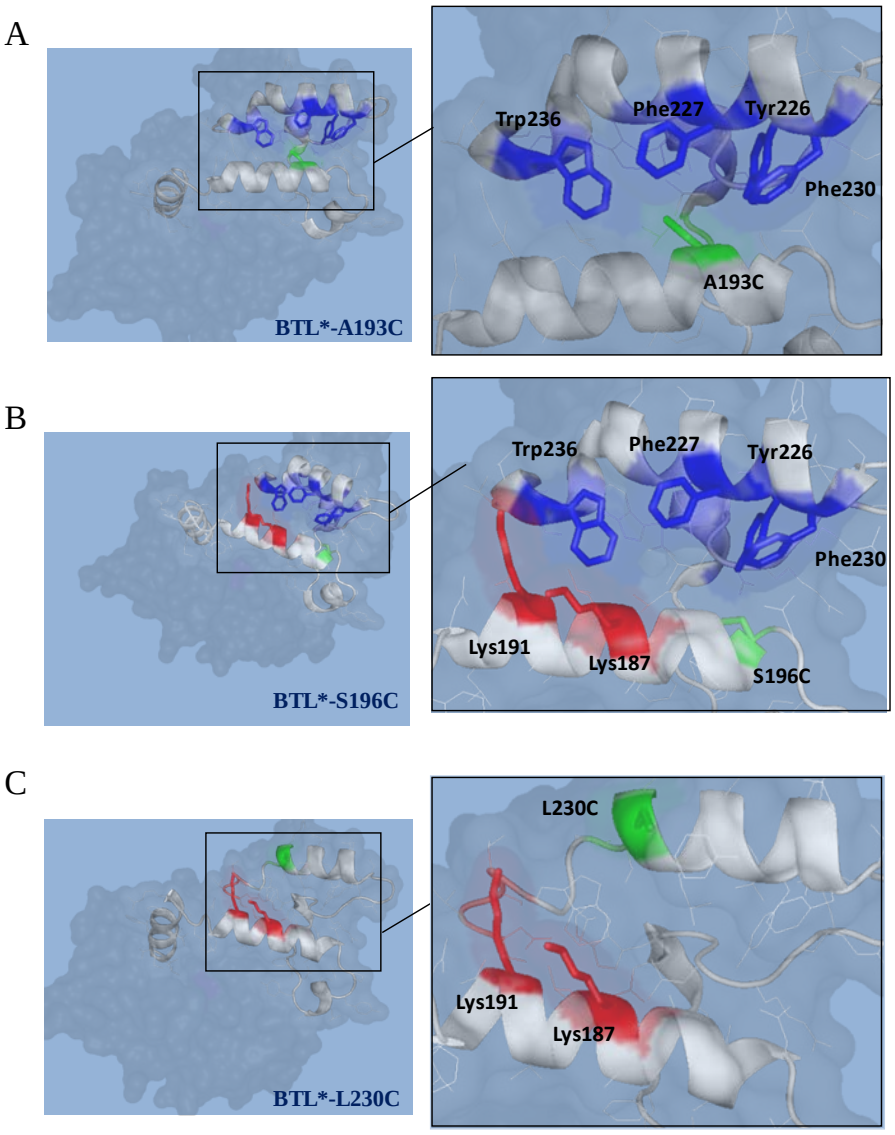

Fig S3. Surface structure of lid zone of BTL mutants. (A) BTL*-A193C; (B) BTL*-S196C; (C) BTL*-L230C. The pdb code for BTL (open conformation) is 2W22.

The first lid is composed principally for aminoacids with cationic residues whereas the second lid is composed with aminoacids with aromatic residues. Therefore, peptide **p1** was introduced on 193 position (first loop) for hydrophobic interactions with the second loop and **p2** was introduced in 230 (loop 2) for electrostatic interactions with the first loop. Both peptides would be complementary peptides for the both loops sequences.

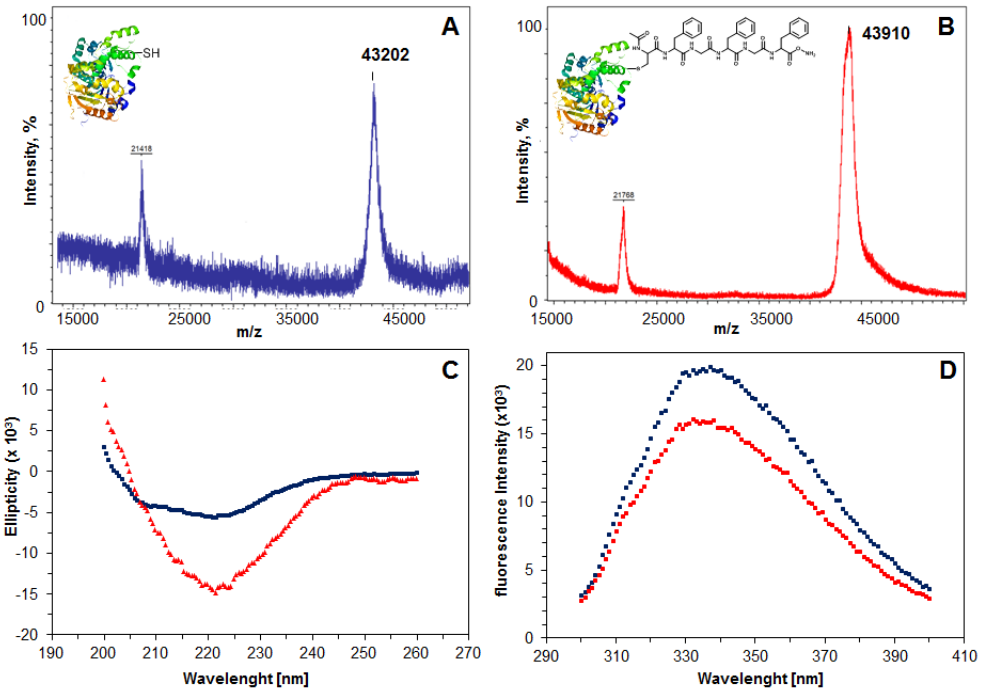

Fig S4. Characterization of BTL*-S196C-p2 conjugate. (A) MALDI-MS spectra of BTL*-S196C, [M+Na]; (B) MALDI-MS spectra of BTL*-S196C-**p2**, [M+Na]; (C) Far-UV CD spectra; (D) Fluorescent spectra. BTL*-S196C (blue), BTL*-S196C-**p2** (red).

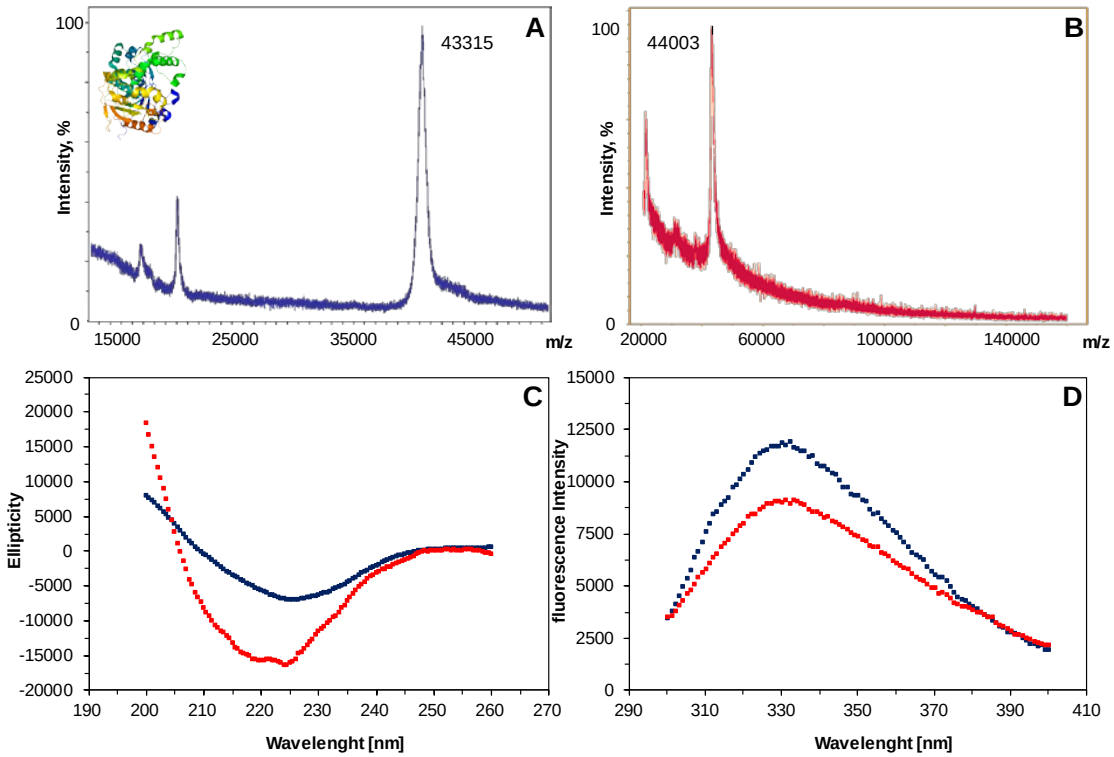

Fig S5. Characterization of BTL*-L230C-p2 conjugate. (A) MALDI-MS spectra of BTL*-L230C, [M+Na]; **(B)** MALDI-MS spectra of BTL*-L230C-**p2**, [M+Na]; **(C)** Far-UV CD spectra; **(D)** Fluorescent spectra. BTL*-L230C variant (blue), BTL*-L230C-**p2** (red).

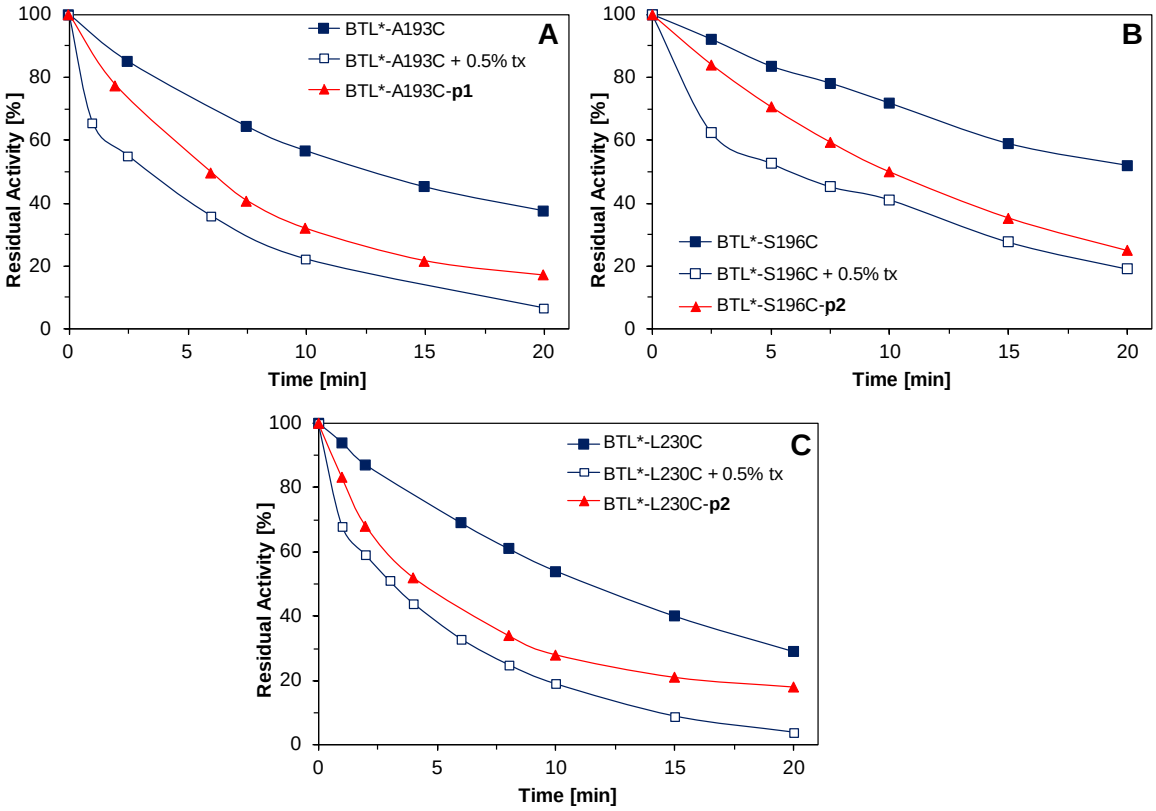

Fig S6. Irreversible inhibition by D-pNP of active sites of different BTL conjugates. (A) BTL*-A193C conjugates; (B) BTL*-S196C conjugates; (C) BTL*-L230C conjugates.

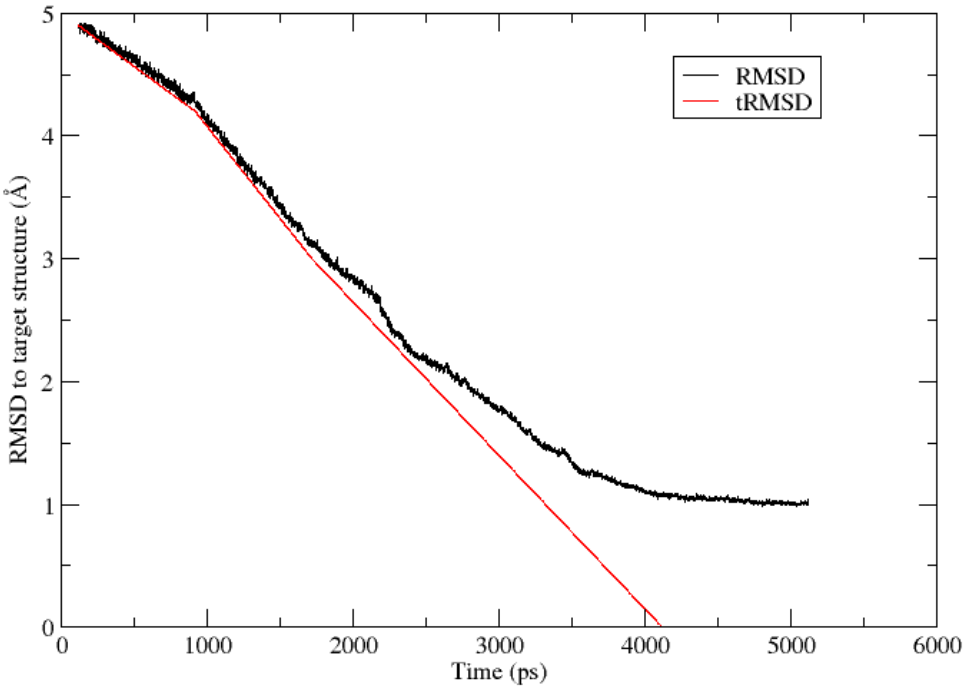

Fig S7. Time-evolution of RMSD (red) and tRMSD (black) values for the Targeted MD of BTL. Evolution from the closed to the open conformation of BTL was followed along 5ns of the targeted MD.

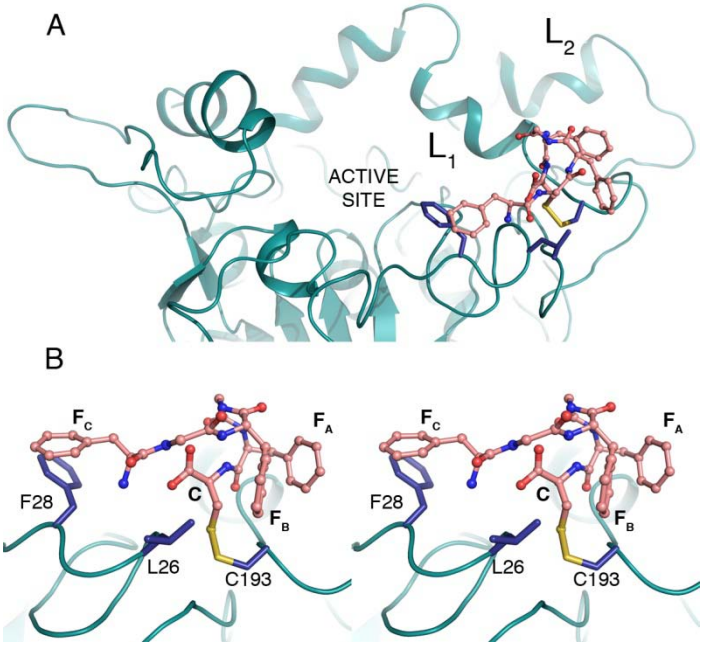

Fig S8. Interaction network of the p1 tag within the modeled structure of the semisynthetic conjugated variant BTL*-A193C-p1. (A) Cartoon representation of the active BTL*-A193C-**p1** variant, showing the relative position of the peptide tag (pink ball and sticks). The tag is accommodated in a hydrophobic patch close to the active site. (B) Stereo view describing the details of the protein-tag interaction. Residues from the enzyme involved in the interaction with the tag are drawn as blue sticks and labeled.

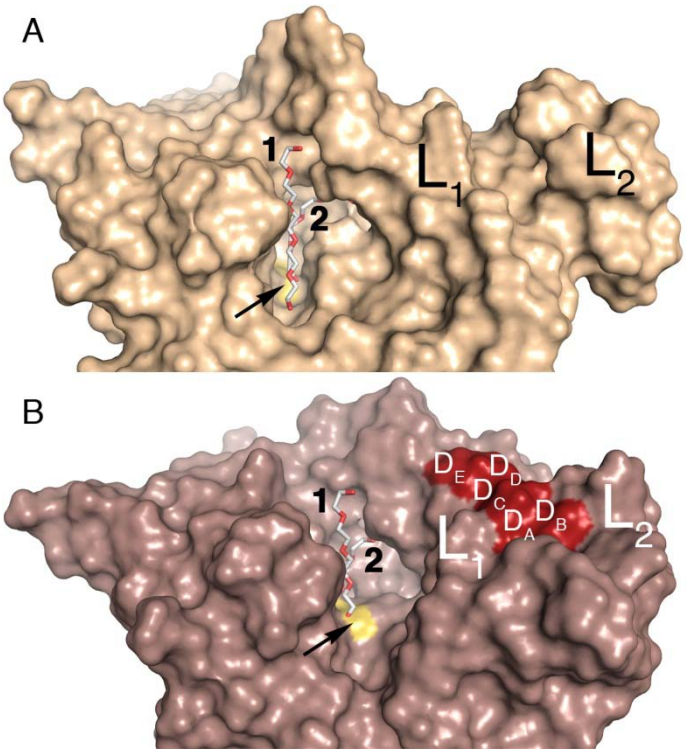

Fig S9. Comparison between the crystal structure of the active form of BTL and the semisynthetic conjugated variant BTL*-S196C-p2. (A) Molecular surface of the BTL crystal structure with the detergent moieties (sticks, 1 and 2) bound into the active site. (B) Molecular surface of active BTL*-S196C-**p2**, with the detergent moieties (from A) superimposed. Aspartic residues (DA-E) from the peptide tag, p2, are highlighted in red. The positions of the lids (L1 and L2) are labeled on the surface. Arrows shows the position of the catalytic Ser114.

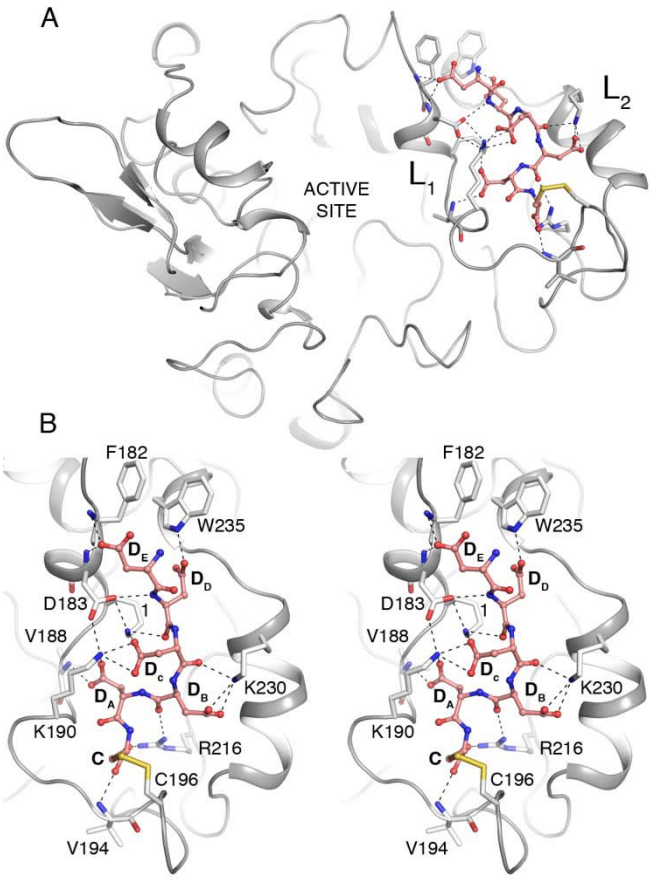

Fig S10. Interaction network of the p2 tag within the modeled structure of the semisynthetic conjugated variant BTL*-S196C-p2. (A) Cartoon representation of the active BTL*-S196C-**p2** variant structure showing the position of the peptide tag (pink ball sticks). The tag is accommodated between the two lids (L1 and L2). (B) Stereo view describing the details of the protein-tag interaction. Salt bridges and hydrogen bonds are showed as dotted lines. Residues from the enzyme involved in the interaction with the tag are drawn as white sticks and labeled. Lys186 is labeled as 1.

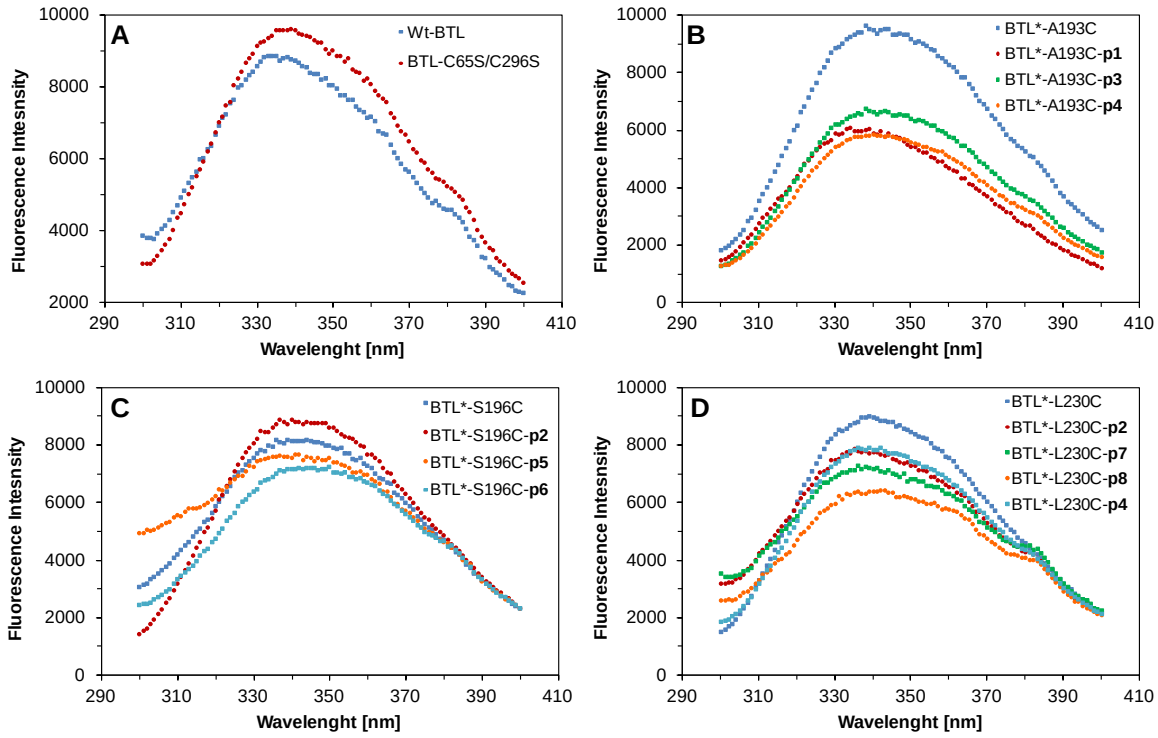

Fig S11. Fluorescence spectra of the immobilized BTL variants. (A) BTL-WT and BTL-C65S/C296S; (B) BTL*-A193C conjugates; (C) BTL*-S196C conjugates; (D) BTL*-L230C conjugates.

Supplementary Tables

Table S1. Primers used to site-directed mutagenesis of BTL.

Mutant [1]	Plasmid template	Primers [2]
C65S C296S *A193C*	pT1BTL2mutCys [3]	Ala/cys 193-5 5´-GAAAGCGtgcGCTGTCGCCAG Ala/cys 193-5 5´- CTGGCGACAGCgcaCGCTTTC
C65S C296S *S196C*	pT1BTL2mutCys	Ser/Cys196-5 5´-GTTGAAAGCGGCGGCTGTCGCCtgcAATGTGCCGTACACGAGTCAAG´ Ser/Cys196-3 5´-CTTGACTCGTGTACGGCACATTgcaGGCGACAGCCGCCGCTTTCAAC
C65S C296S *L230C*	pT1BTL2mutCys	Leu/Cys 230-5 5´-CATTATTTTGAACGGtgcAAACG Leu/Cys 230-3 5´-CGTTTgcaCCGTTCAAAATAATG

[1] The mutant name shows the amino acid changes and its position in BTL.
[2] The nucleotide changes used to introduce the mutation are indicated in lower case
[3] Plasmid with BTL mutant lacking both of the two native Cys residues (Cys65 and Cys 296).

Table S2. Different peptide sequences.

Incorporated peptide	
Ac-Cys-Phe-Gly-Phe-Gly-Phe-$CONH_2$	**p1**
Ac-Cys-$(Asp)_4$-Asp-COOH	**p2**
Ac-Phe-Cys-Phe-Gly-Phe-$CONH_2$	**p3**
Ac-Gly-Gly-Cys-Gly-Gly-$CONH_2$	**p4**
Ac-Cys-$(Arg)_7$-$CONH_2$	**p5**
Ac-Cys-$(Phe\text{-}Gly\text{-})_2$-Asp-Asp-$CONH_2$	**p6**
Ac-Asp-Gly-Asp-Cys-Asp-$CONH_2$	**p7**
Ac-Lys-Gly-Lys-Cys-Lys- $CONH_2$	**p8**

Table S3. Regioselective hydrolysis of peracetylated thymidine 1 catalyzed by peptide-modified immobilized BTL2 mutants at pH 5 and 25ºC.

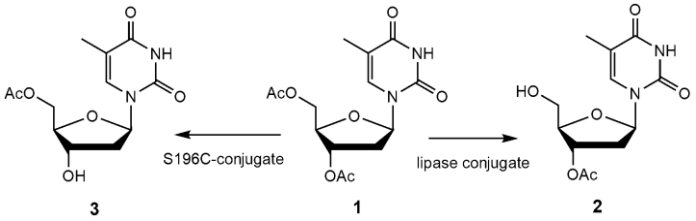

Enzyme	Incorporated peptide	Activity[a]	Time [h]	Yield **2** [%][b]	Yield **3** [%][b]	Thymidine[b]
wt-BTL	-	74	96	65	6	29
BTL-C65S/C296	-	86	80	70	4	26
BTL*-A193C	-	154	72	91	3	6
BTL*-A193C	**p1**	354	48	89	4	7
BTL*-A193C	**p3**	88	96	65	1	34
BTL*-A193C	**p4**	80	96	68	1	31
BTL*-S196C	-	20	50	0	86	14
BTL*-S196C	**p2**	2	100	0	97	3
BTL*-S196C	**p5**	2	100	0	96	4
BTL*-S196C	**p6**	28	48	2	82	16
BTL*-L230C	-	110	69	66	8	26
BTL*-L230C	**p2**	44	162	85	8	7
BTL*-L230C	**p4**	70	162	62	3	35
BTL*-L230C	**p7**	6	192	61	5	34
BTL*-L230C	**p8**	8	96	57	8	35

[a] Specific activity was defined as: $\mu mol.min^{-1}.mg_{lip}^{-1}.10^{-3}$
[b] Yield of the corresponding product at 100% conversion.

Table S4. Regioselective hydrolysis of peracetylated tymidine 1 catalyzed by peptide-modified immobilized BTL2 mutants at pH 7 and 25ºC.

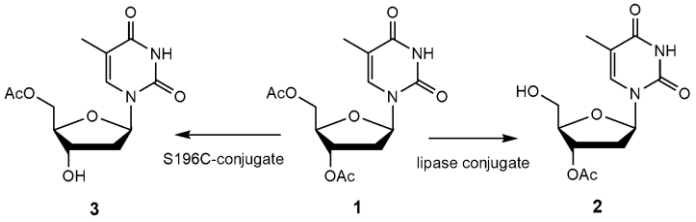

Enzyme	Incorporated peptide	Activity[a]	Time [h]	Yield **2** [%][b]	Yield **3** [%][b]	Thymidine[b]
wt-BTL	**-**	110	80	59	8	33
BTL-C65S/C296S	**-**	130	70	52	4	44
BTL*-A193C	**-**	128	93	79	8	13
BTL*-A193C	**p1**	172	48	88	4	7
BTL*-A193C	**p3**	112	48	44	41	15
BTL*-A193C	**p4**	116	96	33	50	17
BTL*-S196C	**-**	30	30	3	42	55
BTL*-S196C	**p2**	8	44	2	28	70
BTL*-S196C	**p5**	8	44	14	11	75
BTL*-S196C	**p6**	30	48	36	55	9
BTL*-L230C	**-**	154	57	61	14	25
BTL*-L230C	**p2**	86	93	86	4	10
BTL*-L230C	**p4**	186	96	62	2	36
BTL*-L230C	**p7**	2	144	35	37	28
BTL*-L230C	**p8**	4	72	50	30	20

[a] Specific activity was defined as: $\mu molmin^{-1}.mg_{lip}^{-1}.10^{-3}$

[b] Yield of the corresponding product at 100% conversion.

Table S5. Regioselective hydrolysis of peracetylated glucal 4 catalyzed by peptide-modified immobilized BTL2 mutants.

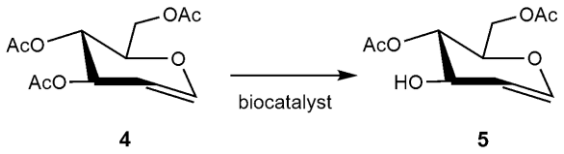

4 **5**

Enzyme[a]	Incorporated peptide	Activity[a]	Time [h]	Yield **5** [%][b]
wt-BTL	-	5	24	72
BTL-C65S/C296S	-	5	24	79
BTL*-A193C	-	183	1	70
BTL*-A193C	**p1**	214	1	73
BTL*-A193C	**p3**	40	5	94
BTL*-A193C	**p4**	79	5	92
BTL*-S196C	-	68	2.5	94
BTL*-S196C	**p2**	2	40	57
BTL*-S196C	**p5**	7	24	77
BTL*-S196C	**p6**	4	24	86
BTL*-L230C	-	98	3	72
BTL*-L230C	**p2**	63	3	50
BTL*-L230C	**p4**	64	5	66
BTL*-L230C	**p7**	6	24	61
BTL*-L230C	**p8**	6	24	67

[a] Specific activity was defined as: $\mu mol.min^{-1}.mg_{lip}^{-1}.10^{-3}$
[b] Yield of the monodeprotected **5** at 100% conversion. The rest of yield corresponds to the bihydrolyzed product

Table S6. Desymmetrization of phenylglutaric acid dimethyl ester catalyzed different BTL-variants at pH 7.0.

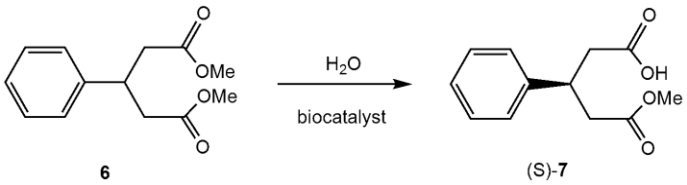

6 (S)-7

Enzyme	Peptide	Activity[a]	Time [h]	*C* [%]	Yield [%][b]	*ee* [%][c]
wt-BTL	-	8.48	196	48	42	68
BTL-C65S/C296S	-	7.61	196	28	23	64
BTL*-A193C	-	0.53	186	23	15	78
BTL*-A193C	**p1**	2.35	96	54	37	>99
BTL*-S196C	-	12.1	50	95	14	94
BTL*-S196C	**p2**	13.3	50	87	21	>99
BTL*-S196C	**p5**	13.4	50	90	25	95
BTL*-L230C	-	11.33	96	65	38	93
BTL*-L230C	**p2**	1.13	96	26	12	73

[a]Specific activity was defined as: $\mu mol.min^{-1}.g^{-1}.10^{-5}$
[b]Yield of the monoester **7**. The rest of conversion corresponds to the dicarboxylic acid.
[c]Determined by HPLC.

Table S7. Kinetic parameters of different BTL immobilized preparations for hydrolysis of *p*NPB at pH 7 and 25 °C.

Enzyme	Peptide	K_m (mM)	V_m (μmol/min)	K_{cat} (s^{-1})
wt-BTL	-	1.23	18.7	2.7
BTL-C65S/C296S	-	1.20	19.3	2.8
BTL*-A193C	-	0.88	18.3	2.6
BTL*-A193C	**p1**	5.75	11.8	1.7
BTL*-S196C	-	0.91	22.0	3.2
BTL*-S196C	**p2**	5.81	34.6	5.0
BTL*-L230C	-	0.76	16.2	2.3
BTL*-L230C	**p2**	2.85	10.4	1.5

MOVIE S1. Targeted-MD: Conformational transition from the closed conformation (PDBID:1ji3) towards the open conformation (PDBID: 2w22) simulated with Targeted Molecular Dynamic of the Amber package. The movie shows the 5ns simulation selecting one snapshot every 5ps, which represents a total of 1000 frames.

MOVIE S2. LES-Simulation: Local Enhanced sampling of the peptide chains attached to the residue 193. The trajectory uses as starting structure the one corresponding to the 3041ps of the targeted-MD. The simulation shows last 200ps selecting one snapshot every 1ps.

MOVIE S3. LES-Simulation: Local Enhanced sampling of the peptide chains attached to the residue 196. The trajectory uses as starting structure the one corresponding to the 2111ps of the targeted-MD. The simulation shows last 200ps selecting one snapshot every 1ps.